Quantification of effects of climate variations and human activities on runoff by a monthly water balance model: A case study of the Chaobai River basin in northern China

Gangsheng Wang,[1,2] Jun Xia,[1,3] and Ji Chen[4]

Received 15 December 2007; revised 23 September 2008; accepted 14 October 2008; published 7 January 2009.

[1] The Chaobai River basin in northern China consists of two major tributaries, the Chao River and Bai River. Monthly observations of precipitation, streamflow, and panevaporation data are available for 35 years (1961–1966 and 1973–2001). Using the annual time series of the observed streamflow, one break point at 1979 is detected and is adopted to divide the data set into two study periods, the "before" and "after" periods marking the onset of significant anthropogenic alteration of the flow (reservoirs and silt retention dams, five times increase in population) and significant changes in land use (conversion to terraced fields versus sloping fields). The distributed time-variant gain model (DTVGM) was used to evaluate the water resources of the area. Furthermore, the Bayesian method used by Engeland et al. (2005) was used in this paper to evaluate two uncertainty sources (i.e., the model parameter and model structure) and for assessing the DTVGM's performance over the Chaobai River basin. Comparing the annual precipitation means over 13 years (1961–1966 and 1973–1979), the means of the second period (1980–2001) decreased by 5.4% and 4.9% in the Chao River and Bai River basins, respectively. However, the related annual runoff decreased by 40.3% and 52.8%, respectively, a much greater decline than exhibited by precipitation. Through the monthly model simulation and the fixing-changing method, it is determined that decreases in runoff between the two periods can be attributed to 35% (31%) from climate variations and 68% (70%) from human activities in the Chao River (Bai River). Thus, human impact exerts a dominant influence upon runoff decline in the Chaobai River basin compared to climate. This study enhances our understanding of the relative roles of climate variations and human activities on runoff.

Citation: Wang, G., J. Xia, and J. Chen (2009), Quantification of effects of climate variations and human activities on runoff by a monthly water balance model: A case study of the Chaobai River basin in northern China, *Water Resour. Res.*, *45*, W00A11, doi:10.1029/2007WR006768.

1. Introduction

[2] Climatic variables, especially rainfall, largely determine the runoff hydrograph of a basin; further, the features of a basin, for example land use/covers, are related to runoff generation. Climate variations may result in changes of the elements of climate, such as precipitation, and human activities can influence drainage basin features [*Beven*, 2001; *Kezer and Matsuyama*, 2006]. Therefore, it is imperative to understand the influence and relative importance of climate variations and human activities on runoff, which is critical to the management of regional water resources. However, quantitative evaluation of the effects of climate variations and human activities on runoff in rivers is still limited. Usually, hydrologic models [*Xu and Vandewiele*, 1995; *Yates*, 1996; *Liu et al.*, 2004; *Chen et al.*, 2007] have been used to investigate the impacts of natural and human factors on the water cycle. In this study, a monthly water balance model is used to investigate the impacts and relative importance of climate variations and human activities on discharge in the Chaobai River in northern China.

[3] In this study, climate variations refer to the changes in precipitation and panevaporation, while the soil and water conservation works (e.g., constructions of reservoir dams and silt retention dams), the regional water demand increases and the land cover changes over the Chaobai River are the mechanisms by which human activities may influence runoff. Presently, techniques for representing the effects of human activities on hydrologic responses are limited. For example, the SCS (Soil Conservation Service) curve number method, developed by the SCS of the USDA (United States Department of Agriculture) [*Thompson*, 1999; *Beven*, 2001], has been widely used for runoff simulations, and can be used for studying the effect of human activities on runoff. The MIKE SHE model, which is also widely used, describes the effects

[1]Key Laboratory of Water Cycle and Related Land Surface Processes, Institute of Geographic Sciences and Natural Resources Research, Chinese Academy of Sciences, Beijing, China.
[2]Department of Biological Systems Engineering, Washington State University, Pullman, Washington, USA.
[3]State Key Laboratory of Water Resources and Hydropower Engineering Sciences, Wuhan University, Wuhan, China.
[4]Department of Civil Engineering, University of Hong Kong, Pokfulam, Hong Kong.

0043-1397/09/2007WR006768

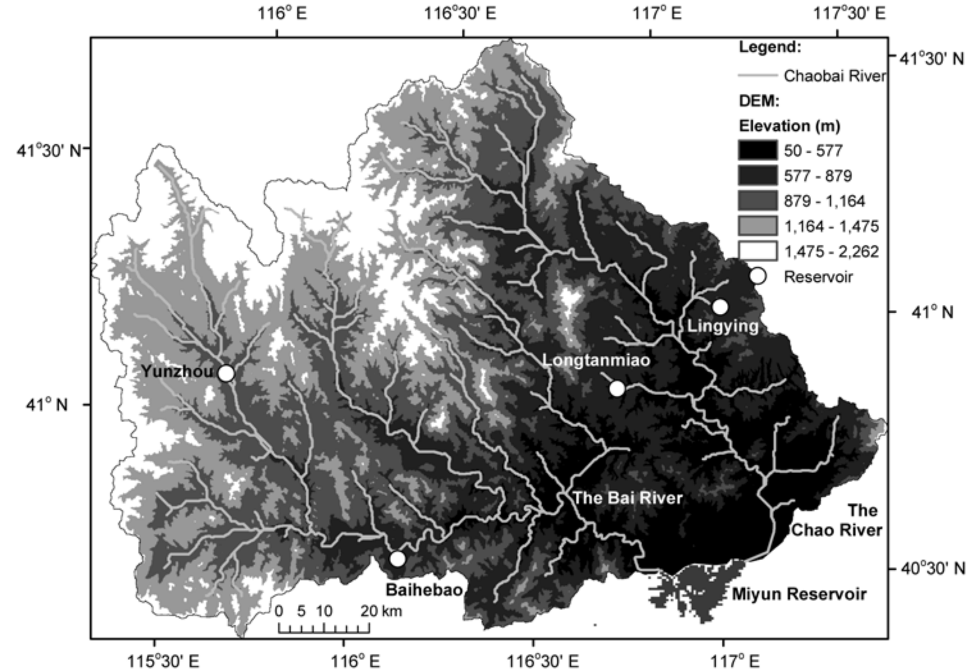

Figure 1. Location of the Chaobai River basin, consisting of the Chao River basin and the Bai River basin, above the Miyun Reservoir in northern China. The locations of the Lingying Reservoir and Longtanmiao Reservoir in the Chao River and the Yunzhou Reservoir and Baihebao Reservoir in the Bai River are marked.

of land use/cover change (LUCC) on the hydrologic process [*Andersen et al.*, 2002]. In a case study on the Qinhuaihe River basin in China, *Wang and Lu* [2003] established the corresponding runoff patterns individually for four different land use types, and analyzed the influences of LUCC on the water resource system.

[4] To simulate runoff rationally, it is crucial to model actual evapotranspiration accurately. Analyzing the hydrometeorological data from 250 basins over the world, *Zhang et al.* [2001] found that a relationship between long-term evapotranspiration and precipitation at the catchment scale existed. In the Bagrov model [*Terpstra and van Mazijk*, 2001], the actual evapotranspiration is calculated from the most important controlling/influencing parameters of precipitation and potential evapotranspiration. Moreover, the Bagrov model employs the effectiveness parameter to reflect the storage properties of the evaporative zone and to indicate the land use and soil type. The monthly water balance model used in this study adopts the Bagrov model for computing the actual evapotranspiration.

[5] Because of concern about water resource sustainability over northern China, numerous studies [e.g., *Liao and Li*, 2003; *Hao*, 2004; *Xia et al.*, 2005] have been undertaken to explore the security of water resources in the region. Specifically, for studying the water resource situation of the Chaobai River basin in northern China, *Wang et al.* [2002] developed the distributed time-variant gain model (DTVGM) to investigate the effect of LUCC on runoff [*Wang et al.*, 2004; *Wang*, 2005]. Using the DTVGM, this study has its objective of quantifying the relative influences of climate variations and human activities upon runoff for the Chaobai River basin. In addition, this study performs an uncertainty analysis of the model si on. Usually, the Bayesian method is used to evaluate uncertainties of hydrologic model simulation [e.g., *Engeland et al.*, 2005; *Yang et al.*, 2007; *Huard and Mailhot*, 2008]. With the Bayesian method used by *Engeland et al.* [2005], two uncertainty sources (i.e., the model parameter and model structure) are studied for assessing the DTVGM's performance over the Chaobai River basin. The results are used to separate the competing influences of climate variations and human activities.

[6] The paper is organized as follows. Section 2 introduces the study area, human activities and data. Sections 3 and 4 describe the model and model parameter optimization and the uncertainty analyses of the model simulation. The results and discussions are presented in section 5.

2. Study Area, Human Activities, and Research Data

2.1. Study Area

[7] The study area is the Chaobai River basin with an area of 13846 km^2 (Figure 1), which is a subbasin of the Hai River basin in northern China. In the basin, currently, forest, grassland, and cultivated land account for 98% of the total area. The river consists of two tributaries, the Chao River and the Bai River, and their confluence is at the Miyun Reservoir, which is the main source of water supply for Beijing City [*Wang and Xia*, 2003]. The Chaobai River basin is delineated into 136 subbasins, with 53 in the Chao River basin and 83 subbasins in the Bai River basin.

2.2. Human Activities

[8] In this study, human activities reflect both direct and indirect influences on runoff. Direct human activities refer to the soil and water conservation works, water demand

increases, and indirect influences include land cover and land use changes over the Chaobai River basin.

[9] Since the late 1970s, China has experienced rapid socioeconomic development, and the regional water consumption and land cover have changed dramatically. According to the land cover maps from the Chinese Academy of Sciences, the coverage of forest increased from 48% in 1980 to 65% in 1995, while grassland and cultivated land decreased from 28% and 22% to 16% and 17%, respectively. More, it is observed that the population over the Chaobai River basin in 1995 was five times that of 1950 (160,000 in 1950, and 870,000 in 1995) [*Liao and Li*, 2003; *Hao*, 2004]. The daily water consumption per capita has been increasing from less than 0.03 m^3 in 1959, to more than 0.10 m^3 in 1995, and to more than 0.20 m^3 in 2000 [*Gao et al.*, 2002; *Chaobai River Management Bureau of Beijing* (*CRMBB*), 2004], and has resulted in a dramatic increase of water.

[10] Over the study area, the regional geography has been changed considerably since 1980 with the sloping fields transformed into terraced fields, and the construction of silt retention dams and some reservoirs (i.e., the soil and water conservation works) in the 1970s and 1980s [*CRMBB*, 2004]. For example, in the Chao River, the Longtanmiao Reservoir with 2.86 million m^3 of storage was built in 1972, and the Lingying Reservoir with 1.44 million m^3 built in 1976. In the Bai River, the Yunzhou Reservoir with 113.7 million m^3 was built in 1970, and the Baihebao Reservoir with 90.6 million m^3 built in 1983 (see Figure 1 for the locations of these reservoirs) [*China Water Yearbook*, 1991]. These reservoirs in the basin are used to store water for agricultural and domestic water demands, which result in not only an enhanced water withdrawing capacity of the local population, but also an increase in total evaporation and leakage from the reservoirs.

[11] Furthermore, silt retention dams constructed in the early 1980s over the Chaobai River basin [*CRMBB*, 2004] have greatly influenced the runoff process. For example, there are two similar small subwatersheds, each with an area of 0.2 km^2, in the Chaobai River basin, one with 23 silt retention dams built around 1980 and the other in a natural condition with no silt retention dams. It was observed that after a rainfall event with 22.4 mm lasting half an hour in July of 2003 no runoff was generated in the first subwatershed but in the second the runoff depth reached 18.5 mm. Therefore, it can be inferred that human activities in the form of silt retention dam construction have the capacity to affect runoff in the Chaobai River.

2.3. Data and Analysis Method

[12] Several data sets were utilized, including a 39-year record of annual precipitation and runoff data (from 1961 to 1966 and 1969 to 2001) and a 35-year record of monthly data including precipitation, runoff and panevaporation (from 1961 to 1966 and 1973 to 2001). In order to detect the changing trends, the Ordered Clustering (OC) analysis method [*Xie et al.*, 2005] is applied in the study. Given a time series $X = \{x_1, x_2, \ldots, x_n\}$, the OC method assumes the possible break point is τ, and then V_τ and $V_{n-\tau}$ are calculated as below:

$$\begin{cases} V_\tau = \sum_{t=1}^{\tau} (x_t - \bar{x}_\tau)^2 \\ V_{n-\tau} = \sum_{t=\tau+1}^{n} (x_t - \bar{x}_{n-\tau})^2 \end{cases} \tag{1}$$

where $\bar{x}_\tau$ and $\bar{x}_{n-\tau}$ are the average values of the two subseries separated at τ. Thus the total sum of the two is given by:

$$S_n(\tau) = V_\tau + V_{n-\tau} \tag{2}$$

The valid break point τ_0 will satisfy the objective function below:

$$S_n(\tau_0) = \min_{2\le\tau\le n-1} \{S_n(\tau)\} \tag{3}$$

3. Monthly Water Balance Model and Human Activities Parameter Set

3.1. Components of Water Balance Model

[13] The distributed monthly water balance model, the DTVGM [*Wang et al.*, 2004], is used over the Chaobai River basin. The water balance in the DTVGM is expressed as below:

$$\Delta AW_t = AW_{t+1} - AW_t = P_t - ETa_t - RS_t - RSS_t - WU_t, \tag{4}$$

where ΔAW is the change of soil moisture storage, AW, in mm. The subscript t and $t+1$ represent variables at time step t and $t+1$, respectively. P is the precipitation, and ETa is the actual evapotranspiration, both in mm. RS and RSS are the surface runoff and subsurface runoff, respectively. WU is the net water consumption, including water use, depression storage, ineffective evapotranspiration (mainly referring to evaporation of irrigation water) and seepage loss. Because of the difficulty of evaluating the value of WU, this study includes WU in the computation of ETa, RS and RSS through adjusting the parameter values related to human activities (see section 3.5 for details).

3.2. Revised Bagrov Evapotranspiration Model

[14] The Bagrov model [*Terpstra and van Mazijk*, 2001] can be applied at the monthly or annual temporal scale, using precipitation to compute evapotranspiration:

$$\frac{dETa}{dP} = 1 - \left(\frac{ETa}{ETp}\right)^N, \tag{5}$$

where ETp is the potential evapotranspiration, and N, the effectiveness coefficient, is an exponential index and is determined by soil and land cover types. Other variables are the same as those used in equation (4). With a boundary condition [*Terpstra and van Mazijk*, 2001], equation (5) can be transformed:

$$d\left(\frac{ETa}{ETp}\right) = \left(1 - \left(\frac{ETa}{ETp}\right)^N\right) \cdot d\left(\frac{P}{ETp}\right), \\ ETa/ETp = 0, \text{ while } P/ETp = 0. \tag{6}$$

In order to estimate the change in evapotranspiration more rationally, in this study, the Bagrov model is revised. In the Bagrov equation, only precipitation is used. However, many studies have indicated that the actual evapotranspiration is considerably influenced by the antecedent soil moisture content [e.g., *Thompson*, 1999; *Davie*, 2002]. Additionally, the boundary condition in equation (6) is not reasonable at the monthly scale, because ETa could not be zero even if there is no precipitation. Therefore, in this study, the soil moisture

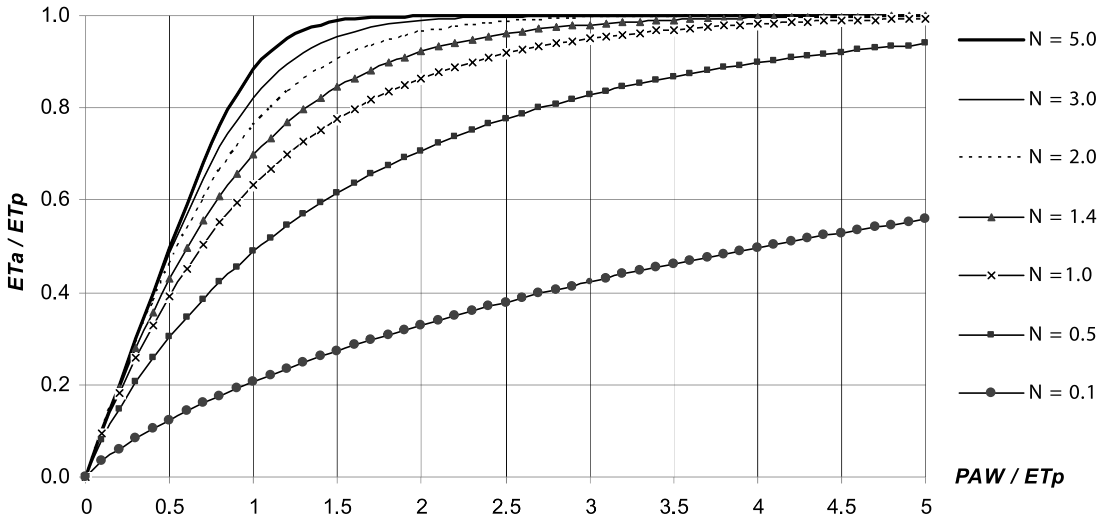

Figure 2. The relationship between *ETa*/*ETp* and *PAW*/*ETp* with different *N*s.

content *AW* is also included in the computation of actual evapotranspiration and the revised Bagrov model is as follows:

$$d\left(\frac{ETa}{ETp}\right) = \left(1 - \left(\frac{ETa}{ETp}\right)^{N}\right) \cdot d\left(\frac{PAW}{ETp}\right),$$
$$ETa/ETp = 0, \text{ while } PAW/ETp = 0, \quad (7)$$

where $PAW = KAW \times (AW + P)$. *KAW* is a coefficient and is determined by model calibration with observed rainfall-runoff data.

[15] Since there is no analytical solution for equation (7), the equation is solved numerically, and the relationship between *ETa*/*ETp* and *PAW*/*ETp* with different *N*s is given in Figure 2. A given value of *N* represents a certain combination of soil and land cover. Generally, according to *Jankiewicz et al.* [2001], the value of *N* is 3.00 for forest, 1.39 for grasslands and 1.63 for cultivated land and bare soil surfaces. With a fixed *N* value, the ratio of *ETa*/*ETp* monotonically increases along with the increase of *PAW*/*ETp*. Figure 2 also shows that with a fixed *PAW*/*ETp*, the higher *N* the higher *ETa*/*ETp*.

3.3. Runoff Simulation

[16] In the DTVGM, the rainfall and antecedent soil moisture content are used to model runoff. The model can be used at daily and monthly scales, and the schemes for computing runoff at the two temporal scales are different. In this study, the scheme at the monthly scale is introduced. Analyzing the observations of runoff and soil moisture over several river basins, *Xia et al.* [2005] found that the surface runoff coefficient is time-variant, and is a function of the antecedent soil moisture content. Therefore, the surface runoff (RS_t) generated in a basin can be described as follows [*Xia et al.*, 2005]:

$$RS_t = g_1 \cdot (AW_t/AWC)^{g_2} \cdot P_t, \quad (8)$$

where g_1 and g_2 are the coefficients, and *AWC* is the saturated soil moisture content.

[17] To model subsurface runoff (RSS_t), there are several methods developed on the of the storage-outflow relationship, including those based on linear, quadratic, power law and exponential relationships [*Lee*, 2007]. In the DTVGM, the RSS_t is calculated by a linear storage-outflow relationship [*Thompson*, 1999; *Lee*, 2007]:

$$RSS_t = Kr \cdot (AW_t + AW_{t+1})/2, \quad (9)$$

where *Kr* is the subsurface runoff coefficient. The rational for using the linear relationship to compute subsurface runoff at the monthly scale will be confirmed in section 5.3 of the paper. Therefore, the total runoff (R_t) generated during month *t* is the sum of surface and subsurface runoff:

$$R_t = RS_t + RSS_t \quad (10)$$

3.4. Model Parameter Optimization

[18] An objective function, *OBF*, is used for identifying the different values of the model parameters for the different periods over the Chao River and Bai River basins. The *OBF* consists of two components: (1) the index of volumetric fit (*IVF*), i.e., the ratio of the simulated runoff volume (VOL_{sim}) to the observed runoff volume (VOL_{obs}), and (2) the Nash-Sutcliffe efficiency criterion (*NSEC*) [*Arnell and Reynard*, 1996]. The equation for computing the *OBF* is:

$$OBF = w \times |1.0 - IVF| + (1.0 - w) \times |1.0 - NSEC|, \quad (11)$$

$$IVF = VOL_{sim}/VOL_{obs}, \quad (12)$$

$$NSEC = 1 - \frac{\sum [Q_{obs}(i) - Q_{sim}(i)]^2}{\sum \left[Q_{obs}(i) - \overline{Q}_{obs}\right]^2}, \quad (13)$$

where *w* is a weighting factor between 0 and 1 (0.5 is used in this study). $Q_{sim}(i)$ and $Q_{obs}(i)$ are the simulated runoff and observed runoff in month *i*. $\overline{Q}_{obs}$ is the observed monthly runoff mean over the study period. This objective function takes account of both volumetric fit and hydrograph fit. When the *OBF* is close to zero (i.e., the values of *IVF* and *NSEC* are closer to 1.0), the model performance is better.

Table 1. Parameter Set Representing Impacts of Human Activities in the Model (HAPS)

Parameter	Note	Lower Bound	Upper Bound
g_1	coefficient of time-variant gain factor, related to surface runoff generation	0.02	0.40
Kr	storage-outflow coefficient related to subsurface runoff generation (1/month)	0.005	0.100
KAW	coefficient for calculating actual evapotranspiration	0.1	1.0

[19] To optimize the value of the *OBF* and to determine the model parameter values at the different periods, the SCE-UA (Shuffled Complex Evolution developed at the University of Arizona) global optimization algorithm [*Duan et al.*, 1992, 1994] is used. The SCE-UA is an integration of four concepts [*Duan et al.*, 1992]: (1) combination of deterministic and probabilistic approaches, (2) systematic evolution of a "complex" of points spanning the parameter space in the direction of global improvement, (3) competitive evolution, and (4) complex shuffling.

[20] Generally, one optimal parameter set can be obtained using such optimization technologies such as the SCE-UA. However, various parameter sets may result in the same objective function value because of the possible existence of the effect of "equifinality" [*Beven and Freer*, 2001; *Beven*, 2001]. To reduce the effect of "equifinality" and to evaluate the model uncertainty influence, it is essential to conduct a model uncertainty analysis using the methods described in the following section.

3.5. Human Activities Parameter Set

[21] Runoff is simulated by the DTVGM [*Wang et al.*, 2004; *Xia et al.*, 2005], and a Human Activities Parameter Set (HAPS) (see Table 1) is used to represent the impacts of human activities on runoff in the model. Intuitively, the impacts of human activities on the terrestrial hydrologic processes can be observed through monitoring various aspects of runoff, evapotranspiration and soil moisture movements. Therefore, some parameters in the DTVGM will be influenced when such impacts are considered in the model, and these are given in Table 1.

[22] In Table 1, the parameter, g_1 used in equation (8), is related to surface runoff, and its value is adjusted during modeling of the influences of human activities (see section 5.4 for the details of why to and how to adjust the parameter's value). The other two parameters, *Kr* in equation (9) and *KAW* in equation (7), represent the influences of human activities through manipulating the soil moisture and evapotranspiration simulation in the model. Usually, the direct effect of human activities is leading the LUCC, and in the DTVGM, parameter *N* in equation (7) can be used to represent the effects of different land covers on evapotranspiration. However, in the study, the value of *N* is fixed according to the suggestions of *Jankiewicz et al.* [2001], and parameter *KAW* is used to represent the influence of the LUCC, since the scale of the LUCC would not change the dominant land cover types, which is used to assign a certain value to *N*, over a region.

[23] Table 1 also lists the lower and upper bounds of the HAPS parameters obtained from both water balance analysis and the model trials. A recent water resources assessment in China gives the mean ratio of surface runoff to precipitation (*RS*/*P*) as 0.16 for North China [*Ministry of Water Resources*, 2007], so the bounds (0.02–0.4) for g_1 in equation (8) should satisfy this requirement over the Chaobai River basin. *KAW* is a coefficient to represent the response of evapotranspiration to the ratio $(AW + P)/ETp$, and it should range from 0 to 1.0. In this study, the range from 0.1 to 1.0 is used since the model trials indicate that *KAW* should not be less than 0.1. The model trials also help to determine that *Kr* has a wide range from 0.005 to 0.100.

4. Model Uncertainty Analysis

[24] To evaluate the effects of climate variations and human activities on hydrologic processes through using the monthly DTVGM model, it is necessary to analyze the uncertainty effects due to the model parameters and the model structure on the model performance. In this paper, such uncertainty analyses over the benchmark period (13 years, 156 months) are conducted using Bayesian inference to analyze the uncertainties of hydrological models [*Engeland et al.*, 2005; *Yang et al.*, 2007]. A brief summary is given below for the purpose of completeness.

[25] Bayes's theorem [*Congdon*, 2001] is applied in this study to explore parameter uncertainty. Using observations q, the posterior distribution $\pi(\gamma, \theta|q)$ of model parameters θ, a vector representing the model parameters, and some statistical parameters γ, a vector describing the simulation errors, can be generated by the prior distribution, $f(\gamma, \theta)$, and the likelihood function of the model, $f(q|\gamma, \theta)$ [*Engeland et al.*, 2005; *Yang et al.*, 2007]:

$$\pi(\gamma, \theta|q) = \frac{f(q|\gamma, \theta) \cdot f(\gamma, \theta)}{\int f(q|\gamma, \theta) \cdot f(\gamma, \theta) \cdot d\gamma \cdot d\theta} \quad (14)$$

where q is a transformation, e.g., $q = \sqrt{Q}$, of the observed model output Q (e.g., runoff) with homoscedastic simulation errors [*Engeland et al.*, 2005].

[26] According to *Engeland et al.* [2005], it can be assumed that $f(\gamma, \theta)$ obeys a uniform distribution and $f(q_t \mid \gamma, \theta)$ follows a normal distribution truncated at zero, thus the likelihood function at time t, $L_t(\gamma, \theta \mid q_t)$ can be written as below:

$$L_t(\gamma, \theta|q_t) = \frac{f(q_t|\gamma, \theta)}{\int_{q_t \geq 0} f(q_t|\gamma, \theta) \cdot d\gamma \cdot d\theta} = \frac{\frac{1}{\sqrt{2\pi\omega_t}} \exp\left[-\frac{(q_t - q_t(\theta))^2}{2\omega_t}\right]}{1.0 - \Phi\left[\frac{-q_t(\theta)}{\sqrt{\omega_t}}\right]} \quad (15)$$

where $q_t(\theta) = \sqrt{Q_t(\theta)}$ and $Q_t(\theta)$ is the simulated runoff depending on the parameter vector θ, ω_t the variance of the simulation error, and Φ the standard cumulative normal distribution [*Engeland et al.*, 2005].

[27] While all the simulation errors are assumed to be independent, the likelihood of the model can be expressed

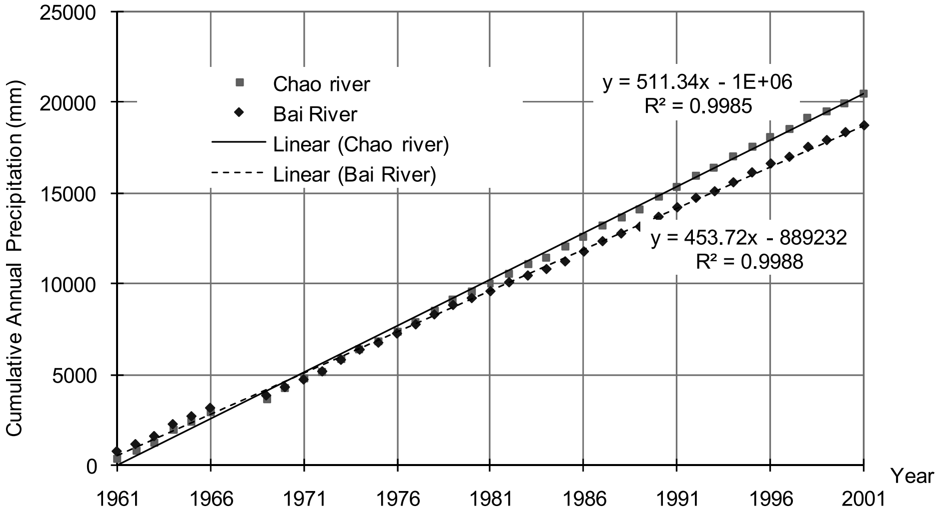

Figure 3. Cumulative annual precipitation from 1961 to 2001 (excluding 1967 and 1968) for the Chao River basin and the Bai River basin.

as the product of the likelihood at each time step [*Engeland et al.*, 2005]:

$$L(\omega, \theta|q) = \prod_{t=1}^{n} L_t(\gamma, \theta|q_t) = \prod_{t=1}^{n} \left\{ \left[1.0 - \Phi\left(-\frac{q_t(\theta)}{\sqrt{\omega_t}}\right)\right]^{-1} \cdot \frac{1}{\sqrt{2\pi\omega_t}} \exp\left[-\frac{(q_t - q_t(\theta))^2}{2\omega_t}\right] \right\} \quad (16)$$

To estimate parameters, the Metropolis Hastings (MH) algorithm, a typical Markov Chain Monte Carlo (MCMC) sampling method [*Engeland et al.*, 2005; *Owen and Tribble*, 2005], is used. The 95% confidence intervals for streamflow due to parameter uncertainty are computed from the streamflow samples with 10000 parameter sets generated by the MH algorithm. According to *Engeland et al.* [2005], the 95% confidence intervals for both the parameter uncertainty and the model structure uncertainty are calculated by adding the model residuals to each of the 10000 streamflow values at each time step, where the residuals are in the form of a random uncertainty with a mean of zero and a standard deviation of ω_t.

5. Results and Discussions

5.1. A Break Point in the Runoff Series

[28] Figures 3 and 4 show the cumulative annual precipitation and runoff over the Chao River and Bai River basins, respectively. Figure 3 shows that the cumulative annual precipitation curves are nearly straight lines, which may infer that there is no abrupt change in the annual precipitation.

[29] Using the OC method (see section 2.3), one break point at 1979 is detected in the runoff record. The significance of this break point is tested using the software of Proc GLM [*SAS Institute Inc.*, 2004], and indicates that the time series of runoff before and after the break point at 1979 are significantly different [*SAS Institute Inc.*, 2004; *Mendenhall and Sincich*, 2007]. Accordingly, the study period is divided into two periods, 1961–19 cluding the period of 1967 to 1972 because of a shortage of monthly data), and 1980–2001 (see Table 2). The mean annual precipitation in the Chao River basin is 511 mm/a and 483 mm/a for the two periods, respectively, and in the Bai River basin it is 471 mm/a and 448 mm/a, respectively, for the corresponding periods.

[30] As per the information of human activities given in section 2.2, it is believed that the break point at 1979 should reflect the changes in the effects of human activities on the water cycle over the basin. For that reason, it would be rational that this study takes the first period (from 1961 to 1966 and 1973 to 1979) as the benchmark period for studying the effects of climate variations and that the effects of human activities on runoff predominated in the second period (from 1980 to 2001).

[31] For investigating the effects of the climate variations on runoff, the corresponding scenario of climate variations (SC) of each period is defined. For example, the SC of DataCPII (see Table 2) refers to the observed precipitation and panevaporation and represents the climate in the Chao River basin at period II. Then, using the SC of DataCPII to replace the SC of DataCPI (the climate conditions during the benchmark period, period I), the effects of climate variations at period II on runoff can be evaluated. Similarly, for example, the HAPS of ParaBPII (Table 2) characterizes the influence of human activities at period II in the Bai River basin, and then the benchmark period of the HAPS may be replaced to explore the influence of human activities at period II. The details of using the SC and HAPS at the different periods for studying the effects of climate variations and human activities on runoff will be presented in section 5.4.

5.2. Uncertainties in Model Parameters and Model Structure

[32] The three HAPS parameters (g_1, *Kr*, and *KAW*) for studying the model parameter uncertainty and the variance of simulation errors (*VAR*) for the model structure uncertainty are involved in the uncertainty estimation. Using the MH method, the 95% confidence intervals of the HAPS parameters in period I and their correlations are computed and these are given in Table 3. Compared with the HAPS parameter ranges in Table 1, all their 95% confidence intervals in Table 3

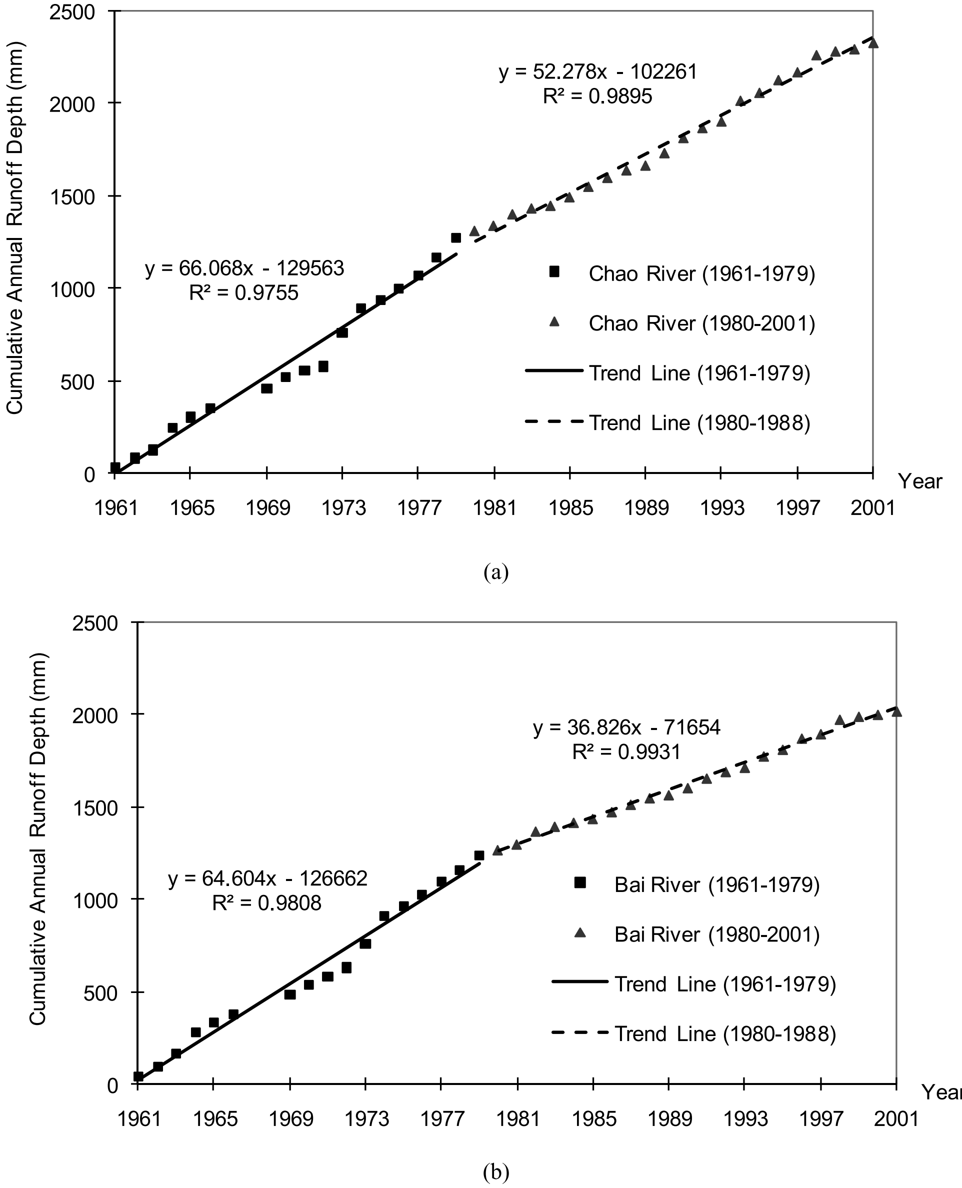

Figure 4. The same as in Figure 3 but for cumulative annual runoff for (a) the Chao River basin and (b) the Bai River Basin.

not only fall within their ranges, but also shrink into much narrower bands. This feature of the 95% intervals reduces the possibility of "equifinality."

[33] In Table 3, it can be observed that the surface runoff parameter, g_1, is negatively related to the subsurface runoff parameter, Kr, whereas Kr is positively related to the evapotranspiration parameter, KAW. However, no correlation is found between g_1 and KAW. These correlations not only corroborate the physical interpretations about the HAPS parameters, but also establish quantitative parameter relationships.

[34] The 95% confidence intervals of the simulated streamflow in period I due to the parameter uncertainty and the model structure uncertainty over the Chao River and the

Table 2. Runoff Simulation Periods and HAPS Referring to the Human Activities-Related Parameter Set[a]

Period	Number of Years	Precipitation (mm/a)		Potential Evapotranspiration (mm/a)		Scenario of Climate Variations (SC)	HAPS
		Chao River	Bai River	Chao River	Bai River		
I: 1961–1966, 1973–1979	13	511	483	1133	1133	DataCPI,[b] DataBPI	ParaCPI, ParaBPI
II: 1980–2001	22	471	448	1096	1264	DataCPII, DataBPII[c]	ParaCPII, ParaBPII

[a]See Table 1.
[b]C and PI in DataCPI denote the Chao River basin and period I, respectively.
[c]B and PII in DataBPII den Bai River basin and period II, respectively.

Table 3. The 95% Confidence Intervals of, and Correlations Between, the HAPS Parameters Estimated by the MH Methods for the Chao River and the Bai River During Period I[a]

	Chao River				Bai River			
	g_1	*Kr*	*KAW*	95% Confidence Interval	g_1	*Kr*	*KAW*	95% Confidence Interval
g_1	1.00	−0.37	0.08	0.046–0.105	1.00	−0.49	0.06	0.032–0.077
Kr	−0.37	1.00	0.64	0.044–0.085	−0.49	1.00	0.46	0.051–0.083
KAW	0.08	0.64	1.00	0.440–0.575	0.06	0.46	1.00	0.355–0.451

[a]MH, Metropolis Hastings.

Bai River are shown in Figures 5 and 6, respectively. From Figures 5a and 6a, it can be found that the influence from the model parameter uncertainty on streamflow simulation is minimal, which further confirms that the possibility of ‘‘equifinality’’ for using the DTVGM would be small. Moreover, the confidence intervals become much wider (Figures 5b and 6b) when the model structure uncertainty is included, which indicates that the uncertainty in streamflow simulation due to the model parameters is less important than that due to the model structure. However, Figures 5b and 6b show that for both basins more than 90% of the observed values are inside the 95% confidence intervals of the simulated streamflow, which indicates that the DTVGM can give robust estimates of the monthly water balance, the long-term average water balance and confidence intervals. The finding from this uncertainty analysis is consistent with that from *Engeland et al.* [2005].

5.3. Monthly Rainfall-Runoff Simulations

[35] Table 4 shows the results of the optimized parameter values at the two study periods for the DTVGM over the Chao River and the Bai River using both the *OBF* and the

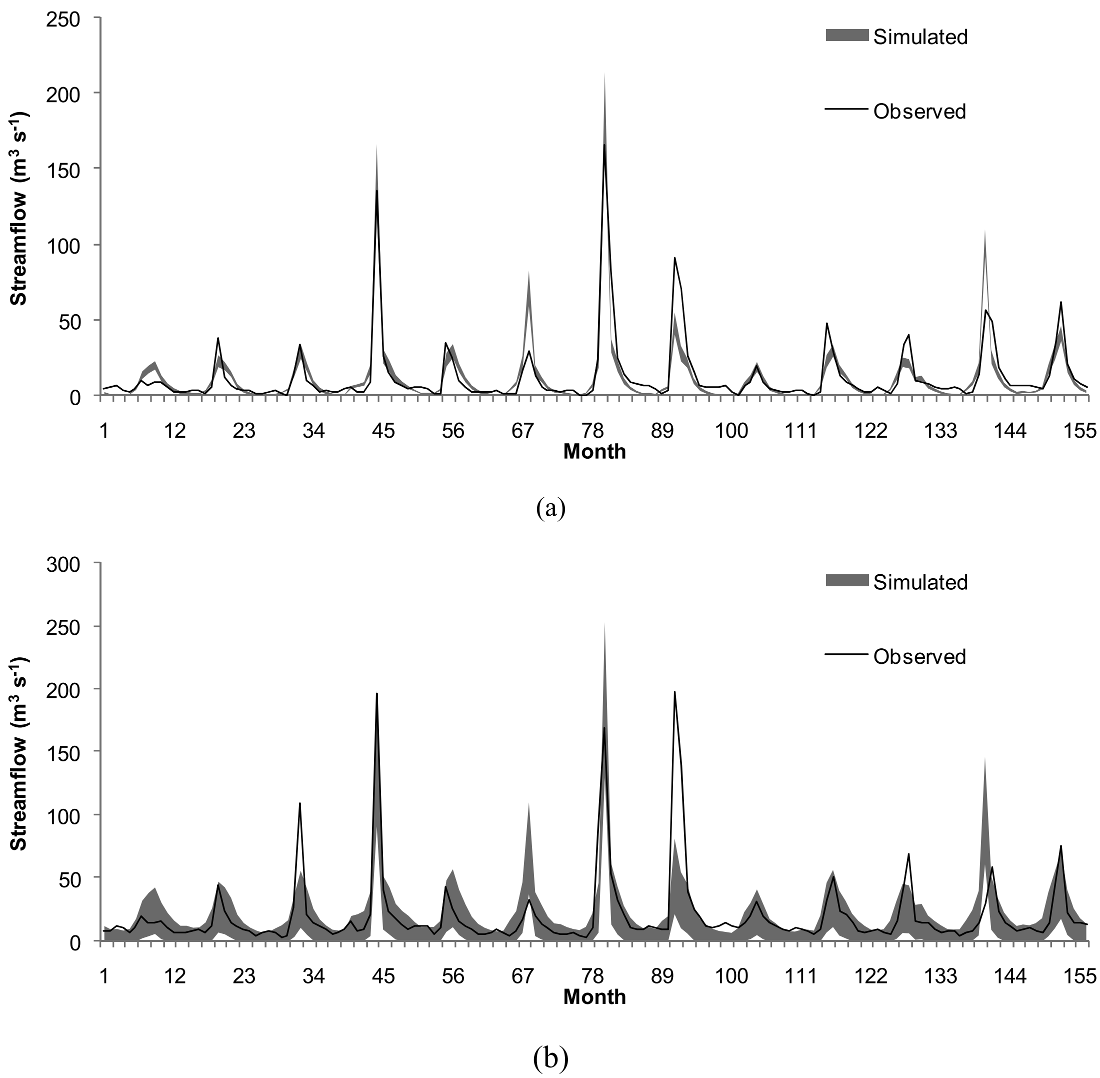

Figure 5. The 95% confidence intervals for simulated streamflow due to (a) the parameter uncertainty and (b) the sum meter and model structure uncertainties in the Chao River basin.

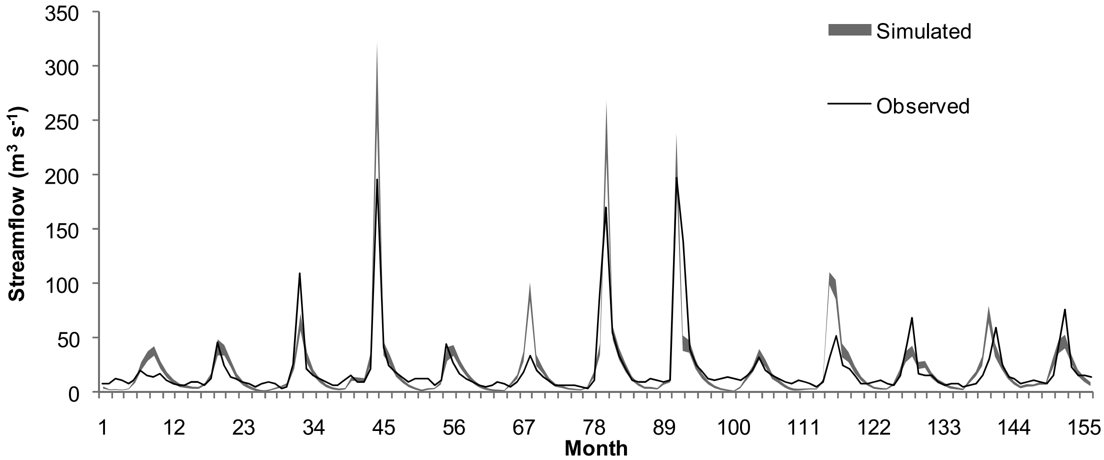

(a)

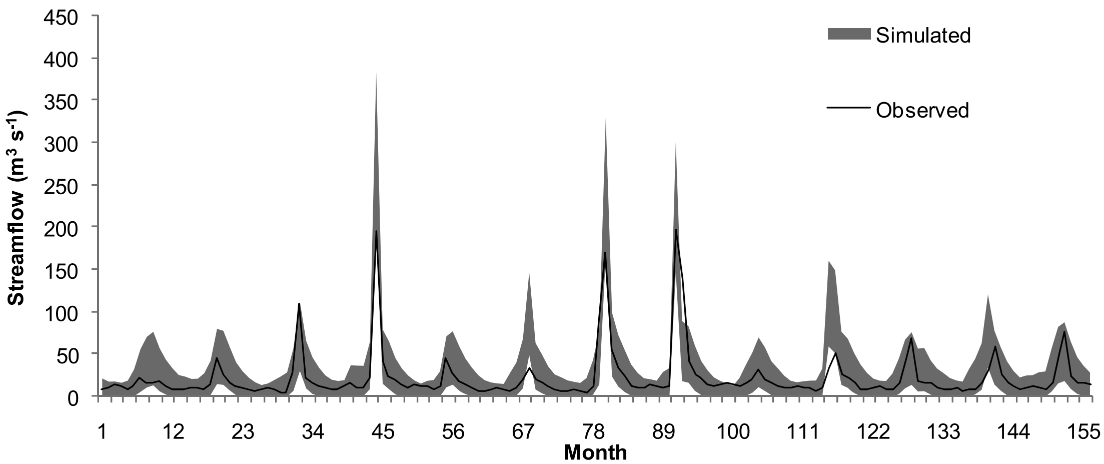

(b)

Figure 6. The same as Figure 5 but for the Bai River basin.

SCE-UA methods. With the optimized *OBF*, Table 4 also gives the results of *IVF* and *NSEC*. From Table 4, it can be observed that HAPS parameter values vary for different time periods. The storage-outflow coefficient *Kr* in period I (see equation (9)), which is related to subsurface runoff generation is smaller than in period II. Meanwhile, the coefficient *KAW* for calculating actual evapotranspiration in equation (7) related to land surface characteristics is larger in period I than in period II over the Chaobai River basin.

[36] As the influence of human activities over the Chaobai River basin was significantly less in the 1960s and 1970s (see section 2.2) [*CRMBB*, 2004; *Hao*, 2004], the rainfall-runoff relationship in period I is selected for studying the effects of human activities occurring at period II. The time-variant gain factor, $G = f(g_1, g_2) = g_1\ (AW/AWC)^{g_2}$, which is the factor for determining the surface runoff generation (see equation (8)) is given in Figure 7. The changes in G are caused by the changes in g_1, and the impact of human activities on surface runoff between two periods can be expressed as:

$$\begin{aligned}\Delta G &= f(g_1', g_2) - f(g_1, g_2)\\ &= (g_1' - g_1) \cdot (AW/AWC)^{g_2} = \Delta g_1 \cdot (AW/AWC)^{g_2},\end{aligned} \qquad (17)$$

where g_1, g_1' are parameter values at the two periods, respectively; Δg_1 is the difference between them. The values of Δg_1 for the Chao River basin and the Bai River basin are -0.010 and -0.033, respectively, which implies that the decreasing trend of surface runoff in the Bai River is larger than that in the Chao River (Figure 7). The changes in the gain factor G and the storage-outflow coefficient Kr given in Table 4 indicate the changes in runoff.

[37] In order to validate the monthly runoff results, the runoff simulations from the DTVGM at a daily scale are investigated, and the base flow component is separated from the streamflow processes to check the proportions of the various runoff components. In the Chao River basin, the mean

Table 4. Optimized Parameter Values at Different Periods for the Chao River and Bai River

HAPS	*IVF*	*NSEC*	g_1	*Kr* (1/month)	*KAW*
ParaCPI	1.00	0.82	0.080	0.080	0.52
ParaCPII	1.00	0.78	0.070	0.050	0.60
ParaBPI	1.00	0.74	0.070	0.072	0.45
ParaBPII	1.00	0.68	0.037	0.041	0.52

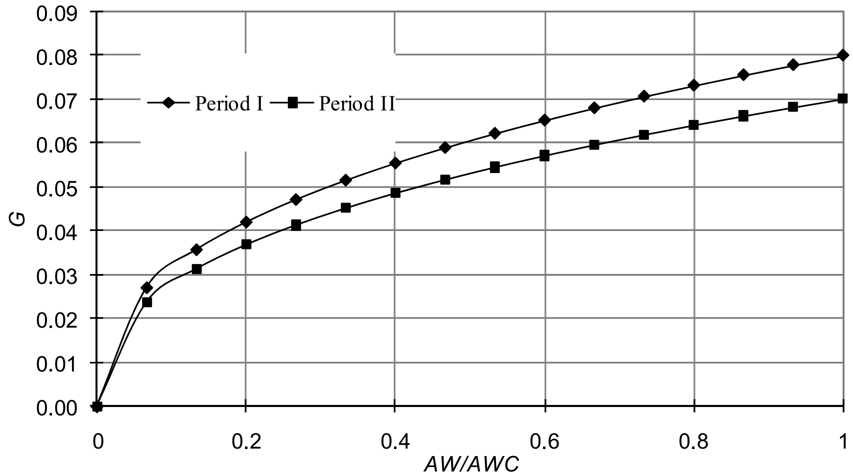

(a)

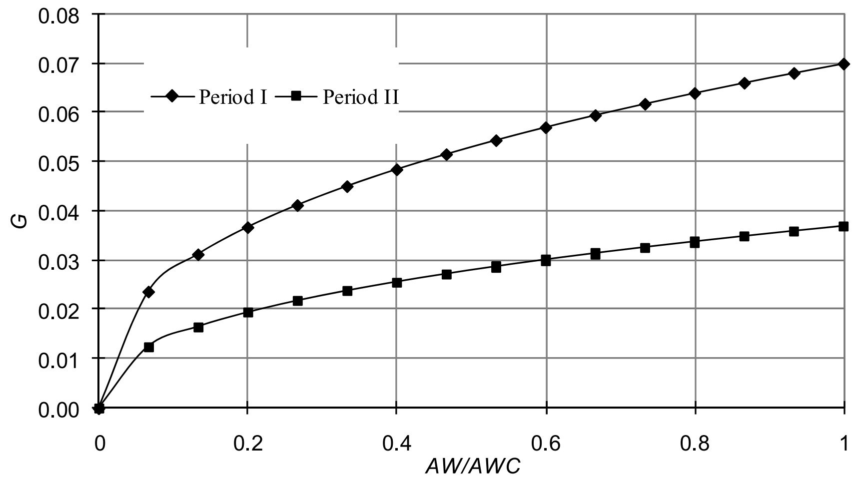

(b)

Figure 7. Relationships between the gain factor (G) and *AW*/*AWC* for different periods for (a) the Chao River basin and (b) the Bai River Basin.

subsurface runoff depth simulated at the monthly scale model is 47.6% of the total runoff during period I, and 43.0% for period II, which are close to the percentage of the subsurface runoff component, 40.1%, at the daily scale model. In the Bai River basin, the ratios of the subsurface runoff to the total runoff in the monthly model are 60.6% and 54.1% for periods I and II, respectively, while this ratio for the daily model is about 53.1%. These ratios of simulated subsurface runoff are in accordance with the results from base flow separation [*Arnold and Allen*, 1999] using daily streamflow data, where the base flow contributed around 45% and 54% to the total runoff in the Chao River and Bai River, respectively. The subsurface runoff at the monthly scale with a linear storage-outflow relation (see equation (9)) is close to that at the daily scale, which indicates that such a linear description for the subsurface runoff at the monthly scale is valid.

5.4. Impacts of Climate Variations and Human Activities on Runoff

[38] To evaluate the relative contributions of climate variations and human activities to the changes in runoff, the fixing-changing method [*Zhang*, 2004] is adopted to run the DTVGM. The fixing-cha factor technique involves fixing one factor and changing another factor to assess the effects of the changed factor on model performance. In this study, the influences of climate variations and human activities are investigated. Table 5 gives the contribution rates (*CR*) of the two factors to the changes of runoff over the Chao River and Bai River.

[39] The *CR* is computed on the basis of the differences of runoff simulation using SC and HAPS at different periods. For example, for assessing the effects of human activities at period II at the Chao River basin, the runoff simulations using three pairs of SC and HAPS, (pair one: DataCPI and ParaCPI in period I, pair two: DataCPII and ParaCPII in period II, and pair three: DataCPI and ParaCPII) are processed. Then, in the Chao River, the *CR* of the effects of human activities at period II is computed as follows:

$$CR(\text{human activities, Period II}) = \frac{R(\text{DataCPI, ParaCPII}) - R(\text{DataCPI, ParaCPI})}{R(\text{DataCPII, ParaCPII}) - R(\text{DataCPI, ParaCPI})} \times 100\% \qquad (18)$$

[40] Table 5 shows that when the SC is DataCPI and the HAPS is ParaCPII, the simulated runoff is 56.80 mm/a.

Table 5. Contribution of Climate Variations and Human Activities to the Changes of Runoff

Period	Variable and Parameter	Precipitation (mm/a)	Runoff (mm/a) Obs	Runoff (mm/a) Sim	Diff = Sim − Sim(I) (mm/a)	Contribution Ratio (%)
			Chao River Basin			
I	DataCPI, ParaCPI	510.69	78.48	78.55	0	0
Human influence	DataCPI, ParaCPII	510.69		56.80	−21.75	68.6
Climate impact	DataCPII, ParaCPI	483.01		67.43	−11.12	35.1
II	DataCPII, ParaCPII	483.01	46.84	46.83	−31.72	100
			Bai River Basin			
I	DataBPI, ParaBPI	471.37	74.12	74.12	0	0
Human influence	DataBPI, ParaBPII	471.37		46.77	−27.35	70.4
Climate impact	DataBPII, ParaBPI	448.27		62.21	−11.91	30.7
II	DataBPII, ParaBPII	448.27	34.97	35.27	−38.85	100

Using equation (18), the *CR* is 68.6%, and it would be interpreted that the contribution of human activities to the runoff decrease at period II is 68.6%. Similarly, for evaluating the influence of climate variations, the runoff simulation using the pair of ParaCPI and DataCPII is processed, and the simulated runoff is 67.43 mm/a (see Table 5). Using equation (18), the *CR* is 35.1%, and consequently the contribution of climate variations at period II to runoff change is 35.1%.

[41] Table 5 also reveals the total runoff change from period I to period II is −31.72 mm/a over the Chao River basin; however, the contributions of human activities and climate variations to this runoff change are −21.75 mm/a and −11.12 mm/a, respectively. There is a residual of 1.15(=−31.72 − (−21.75 − 11.12)) mm/a, which is caused by simultaneous changes of the SC and the HAPS and the nonlinear features of the model in simulating runoff (see section 3.3). This explains why the sum of the *CR*s of climate variations and human activities to the runoff decrease is not equal to 100% (68.6% + 35.1% = 103.7%).

[42] Correspondingly, comparisons from Table 5 between periods I and II in the Bai River basin show that the *CR*s of climate variations and human activities to runoff decrease are 30.7% and 70.4%, respectively. Generally, the influence of human activities on runoff over the Chaobai River basin is about twice that of climate variations, and the effect of human activities on runoff decrease in the Bai River is slightly greater than that in the Chao River. At the two study periods (1961–1966 and 1973–1979 against 1980–2001), the runoff coefficients in the Chao River basin are 0.15 and 0.10, and in the Bai River basin are 0.16 and 0.08, respectively. These changes of runoff coefficients would reflect the influence of human activities on runoff.

6. Conclusions

[43] A monthly water balance model was used to evaluate the impacts of climate variations and human activities on the changes of runoff in the Chaobai River basin in northern China. In the model, three parameters, g_1, *Kr*, and *KAW*, represent the effects of human activities. The responses of streamflow to the uncertainties in model parameters and model structure are estimated using the Bayesian method, and it is found that the uncertainty in streamflow simulation due to the model parameters is less important than uncertainty due to the model structure. The uncertainty analysis indicates that the monthly model can consistently simulate the hydrologic processes over the study area. Finally, the relative contribution of climate variations and human activities to runoff change are evaluated using the fixing-changing factor technique.

[44] Using the observed monthly streamflow and rainfall over a period of 35 years (1961–1966, 1973–2001) from the Chao River and Bai River to drive the monthly water balance model, the 35-year period is separated into period I (1961–1966 and 1973–1979) and period II (1980–2001) according to a break point in the observational record that is detected at 1979. Over the Chao River and Bai River basins, the changes in runoff from period I to period II are much larger than the changes in rainfall. The difference between the rainfall and runoff between the two periods indicates the effects of human activities on runoff. This study revealed that the contribution of human activities to the decrease in runoff is 68.6% in the Chao River basin (70.4% in the Bai River basin). Therefore, it is inferred that human activities are the main cause of runoff decrease over the Chaobai River basin in the 1980s and the 1990s.

[45] **Acknowledgments.** This research was supported by the National Natural Science Foundation of China (40730632/40671035), the President's Award Special Fund of the Chinese Academy of Sciences, and the Special Fund of the Ministry of Science and Technology, China (2006DFA21890). The authors are also grateful for the valuable review comments and suggestions from the three anonymous reviewers.

References

Andersen, J., G. Dybkjaer, K. H. Jensen, J. C. Refsgaard, and K. Rasmussen (2002), Use of remotely sensed precipitation and leaf area index in a distributed hydrological model, *J. Hydrol.*, *264*, 34–50, doi:10.1016/S0022-1694(02)00046-X.

Arnell, N. W., and N. S. Reynard (1996), The effects of climate change due to global warming on river flows in Great Britain, *J. Hydrol.*, *183*(3–4), 397–424, doi:10.1016/0022-1694(95)02950-8.

Arnold, J. G., and P. M. Allen (1999), Automated methods for estimating baseflow and ground water recharge from streamflow records, *J. Am. Water Resour. Assoc.*, *35*(2), 411–424, doi:10.1111/j.1752-1688.1999.tb03599.x.

Beven, K. J. (2001), *Rainfall-Runoff Modeling*, 360 pp., John Wiley, Chichester, U. K.

Beven, K., and J. Freer (2001), Equifinality, data assimilation, and uncertainty estimation in mechanistic modelling of complex environmental systems using the GLUE methodology, *J. Hydrol.*, *249*(1–4), 11–29, doi:10.1016/S0022-1694(01)00421-8.

Chaobai River Management Bureau of Beijing (2004), *Flood and Drought Hazards in the Chaobai River* (in Chinese), 209 pp., China Water Resour. and Hydropow. Press, Beijing.

Chen, X., Y. D. Chen, and C. Y. Xu (2007), A distributed monthly hydrological model for integrating spatial variations of basin topography and rainfall, *Hydrol. Processes*, *21*, 242–252, doi:10.1002/hyp.6187.

China Water Yearbook (1991), *Hai River Basin* (in Chinese), Hebei Hydrol. Stn., Shijiazhuang, China.
Congdon, P. (2001), *Bayesian Statistical Modelling*, 531 pp., John Wiley, Chichester, U. K.
Davie, T. (2002), *Fundamentals of Hydrology*, pp. 30–42, Routledge, New York.
Duan, Q., S. Sorooshian, and V. K. Gupta (1992), Effective and efficient global optimization for conceptual rainfall-runoff models, *Water Resour. Res.*, *28*(4), 1015–1031, doi:10.1029/91WR02985.
Duan, Q., S. Sorooshian, and V. K. Gupta (1994), Optimal use of the SCE-UA global optimization method for calibrating watershed models, *J. Hydrol.*, *158*, 265–284, doi:10.1016/0022-1694(94)90057-4.
Engeland, K., C.-Y. Xu, and L. Gottschalk (2005), Assessing uncertainties in a conceptual water balance model using Bayesian methodology, *Hydrol. Sci. J.*, *50*(1), 45–63, doi:10.1623/hysj.50.1.45.56334.
Gao, Y. C., Z. J. Yao, B. Q. Liu, and A. F. Lv (2002), Evolution trend of Miyun Reservoir inflow and its motivating factors analysis (in Chinese), *Prog. Geogr.*, *21*(6), 546–553.
Hao, L. J. (2004), Analysis on variation and influencing factors of rainfall-runoff relationship in Miyun Reservoir watershed (in Chinese), *Beijing Water Resour.*, *3*, 41–43.
Huard, D., and A. Mailhot (2008), Calibration of hydrological model GR2M using Bayesian uncertainty analysis, *Water Resour. Res.*, *44*, W02424, doi:10.1029/2007WR005949.
Jankiewicz, P., G. Glugla, and C. Rachimow (2001), The mean annual actual evapotranspiration (in German), in *Hydrological Atlas of Germany (1961–1990)* [electronic], Fed. Inst. for Hydrol., Berlin.
Kezer, K., and H. Matsuyama (2006), Decrease of river runoff in the Lake Balkhash basin in central Asia, *Hydrol. Processes*, *20*(6), 1407–1423, doi:10.1002/hyp.6097.
Lee, D. H. (2007), Testing a conceptual hillslope recession model based on the storage-discharge relationship with the Richards equation, *Hydrol. Processes*, *21*, 3155–3161.
Liao, R. H., and Q. J. Li (2003), Studies on river basin sustainable development strategy for the Miyun Reservoir (in Chinese), *China Water Resour.*, *8*, 22–23.
Liu, C. M., J. Xia, and S. L. Guo (2004), Advances in distributed hydrological modeling in the Yellow River Basin (in Chinese), *Adv. Water Sci.*, *15*(4), 495–500.
Mendenhall, W., and T. Sincich (2007), *Statistics for Engineering and the Sciences*, 5th ed., 1060 pp., Prentice Hall, Upper Saddle River, N. J.
Ministry of Water Resources (2007), *China Water Resources Assessment* (in Chinese), Beijing.
Owen, A. B., and S. D. Tribble (2005), A quasi-Monte Carlo Metropolis algorithm, *Proc. Natl. Acad. Sci. U. S. A.*, *102*(25), 8844–8849, doi:10.1073/pnas.0409596102.
SAS Institute Inc (2004), *Basic Getting Started Guide for SAS 9.1.2*, Cary, N. C.
Terpstra, J., and A. van Mazijk (2001), Computer aided evaluation of planning scenarios to assess the impact of land-use changes on water balance, *Phys. Chem. Earth B*, *26*(7–8), 523–527.
Thompson, S. A. (1999), *Hydrology for Water Management*, 362 pp., A. A. Balkema, Rotterdam, Netherlands.
Wang, G. S. (2005), Theory and method of distributed time-variant gain model (in Chinese), doctoral thesis, Grad. Sch. of the Chin. Acad. of Sci., Beijing.
Wang, J. Q., and Z. H. Lu (2003), Study on the impact of land use changes on the hydrological system (in Chinese), *Adv. Earth Sci.*, *18*(2), 292–298.
Wang, G. S., and J. Xia (2003), Sustainable water resources exploitation and management in Beijing, in *Sustainable Water Management Solutions for Large Cities (the 23rd General Assembly of IUGG)*, edited by D. A. Savic et al., *IAHS Publ.*, *293*, 90–93.
Wang, G. S., J. Xia, G. Tan, and A.-F. Lu (2002), A research on distributed time variant gain model: A case study on Chao River basin (in Chinese), *Prog. Geogr.*, *21*(6), 573–582.
Wang, G. S., J. Xia, Y.-Z. Zhu, C.-W. Niu, and G. Tan (2004), Distributed hydrological modeling based on nonlinear system approach (in Chinese), *Adv. Water Sci.*, *15*(4), 521–525.
Xia, J., M. Y. Liu, S. F. Jia, and X. F. Song (2005), Water security problem in north China: Research and perspective, *Pedosphere*, *15*(5), 563–575.
Xie, P., G. C. Chen, D. Li, and Y. Zhu (2005), Comprehensive diagnosis method of hydrologic time series change-point analysis (in Chinese), *Water Resour. Pow.*, *23*(2), 11–14.
Xu, C. Y., and G. L. Vandewiele (1995), Parsimonious monthly rainfall-runoff models for humid basins with different input requirements, *Adv. Water Resour.*, *18*, 39–48, doi:10.1016/0309-1708(94)00017-Y.
Yang, J., P. Reichert, and K. C. Abbaspour (2007), Bayesian uncertainty analysis in distributed hydrologic modeling: A case study in the Thur River basin (Switzerland), *Water Resour. Res.*, *43*, W10401, doi:10.1029/2006WR005497.
Yates, D. N. (1996), WatBal: An integrated water balance model for climate impact assessment of river basin runoff, *Water Resour. Dev.*, *12*(2), 121–139, doi:10.1080/07900629650041902.
Zhang, L. N. (2004), Analysis and simulation of hydrological impacts of land cover changes on the Bai River Basin (in Chinese), doctoral thesis, Grad. Sch. of the Chin. Acad. of Sci., Beijing.
Zhang, L., W. R. Dawes, and G. R. Walker (2001), Response of mean annual evapotranspiration to vegetation changes at catchment scale, *Water Resour. Res.*, *37*(3), 701–708, doi:10.1029/2000WR900325.

J. Chen, Department of Civil Engineering, University of Hong Kong, Pokfulam Road, Pokfulam, Hong Kong.

G. Wang, Department of Biological Systems Engineering, Washington State University, Pullman, WA 99164-6120, USA.

J. Xia, Key Laboratory of Water Cycle and Related Land Surface Processes, Institute of Geographic Sciences and Natural Resources Research, Chinese Academy of Sciences, Beijing 100101, China. (xiaj@igsnrr.ac.cn)